A Low-profile Miniaturized Second-Order Bandpass Frequency Selective Surface

Muaad Hussein, Jiafeng Zhou, Yi Huang and Bahaa Al-Juboori

***Abstract*- High order bandpass frequency selective surfaces (FSSs) (N ≥ 1) can achieve high performance with a flat in-band frequency response and fast roll-off. One particular practical issue of designing bandpass FSSs using resonant surfaces is that the thickness of the substrate would be around a quarter of wavelength. On the other hand, the size of a non-resonant FSS array element is usually large. A new miniaturized FSS capable of exhibiting a second order bandpass response is proposed in this paper. Two miniaturized resonant surfaces coupled by a non-resonant inductive layer are used to build the proposed FSSs. An FSS operating at around 3.8 GHz is designed to verify the method. The element size is smaller than 0.076λ×0.076λ for the proposed structure. This is significantly smaller than the element size of second-order FSSs designed using conventional approaches. The overall thickness is less than λ/24, where λ is the free space wavelength at the resonant frequency. The method could be particularly useful for the design of FSSs at lower frequencies with longer wavelengths.**

***Index Terms*— Array element, bandpass filter, frequency selective surfaces (FSS), miniaturization, periodic structures, radome.**

I. INTRODUCTION

FSSs with bandpass performances have gained more and more attention recently. Many design methods and structures have been adopted to obtain bandpass responses. In order to achieve a bandpass response with an almost flat top and a fast roll off, two or more metallic layers can be cascaded to realize the filter. Although theoretically similar to a classical microwave filter, a spatial filter is more complicated. A classical filter has a pair of terminals (input and output). The response is recorded at the output when a signal is fed to the input terminal. A spatial filter has a wave arriving at variable incident angles as well as polarizations. This fact has major impact on the transmission responses. Also FSSs have finite dimensions. The desired frequency selective response can only be observed when the finite surface includes a sufficient number of constituting elements and is illuminated by a planar phase front. For some applications, such as low-frequency antenna radomes, FSSs with array elements of relatively small electrical dimensions are highly desirable because they are less sensitive to the angle of incidence and can operate for non-planar phase fronts.

A spatial bandpass filter can be built by cascading two or more surfaces isolated by dielectric slabs. The thickness of the dielectric slabs is usually around a quarter of wavelength to obtain flat frequency response and fast roll-off [1]. As a result, the structure will be bulky, and sensitive to the wave incident angle, especial for low frequency applications. Using non-resonant traditional patch and mesh to design a low-profile second order bandpass FSS was given in [2] and a miniaturized dual-band FSS in [3]. However, using non-resonant layers could affect the miniaturization of the array elements. A second order bandpass FSS with narrowband responses by using inductively coupled miniaturized element is reported in [4].

In this paper, two resonant miniaturized layers are used as resonators. They are inductively coupled to exhibit a second order bandpass response. The performance is polarization independent and stable at different incident angles. The structure is low-profile and extremely compact, which can be potentially applied for very low frequency applications.

II. THE PROPOSED STRUCTURE

Fig. 1 shows the proposed structure with three surface layers. Two dielectric slabs are used to separate them. The first and third surface layers, as introduced in [5], are identical. They are formed by four stepped-impedance transmission lines connected to a square ring. The middle layer is built using cross dipoles to present inductance. Two dielectric slabs of FR4 with a thickness of 1.6 mm and a dielectric constant ε_r of 4.3 were used to separate the three metallic layers.

For normal incident waves, the equivalent circuit as shown in Fig. 2 can be used to explain the operation principles of the proposed structure. The dielectric slabs, separating the surfaces layers, can be represented by two short pieces of transmission lines h_1 and h_2. The characteristic impedance of the transmission lines is $Z_d = Z_o/\sqrt{\varepsilon_r}$, where Z_o is the free space impedance. In Fig. 2(a), C_1 and C_3 represent the mutual capacitance between adjacent elements in the first and third layers, respectively. C_2 and C_4 represent the capacitance between the patches of an element in the first and third layers, respectively. L_1 represents the inductance of strips on the first layer which are parallel to the E-field, and L_3 represents the inductance of strips on the third layer. L_2 represents the inductance of the inductive layer (the middle layer). The short transmission line sections, h_1 and h_2 in Fig. 2(a), can be replaced with their equivalent circuit model [6] which consists of a shunt capacitor and a series inductor. The revised equivalent circuit is shown in Fig. 2(b).

Manuscript received April 3, 2017; revised April 22, 2017 and August 3, 2017; accepted August 24, 2017. (Corresponding author: Jiafeng Zhou.)

The authors are with the Department of Electrical Engineering and Electronics, The University of Liverpool, Liverpool L69 3GJ, U.K. (e-mail: Jiafeng.Zhou@liverpool.ac.uk).

This article has been accepted for publication in a future issue of this journal, but has not been fully edited. Content may change prior to final publication. Citation information: DOI 10.1109/LAWP.2017.2746266, IEEE Antennas and Wireless Propagation Letters

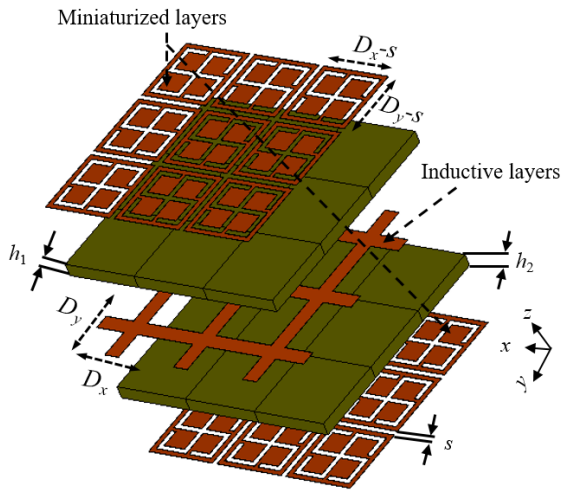

Fig. 1. Topology of the proposed second-order bandpass FSS.

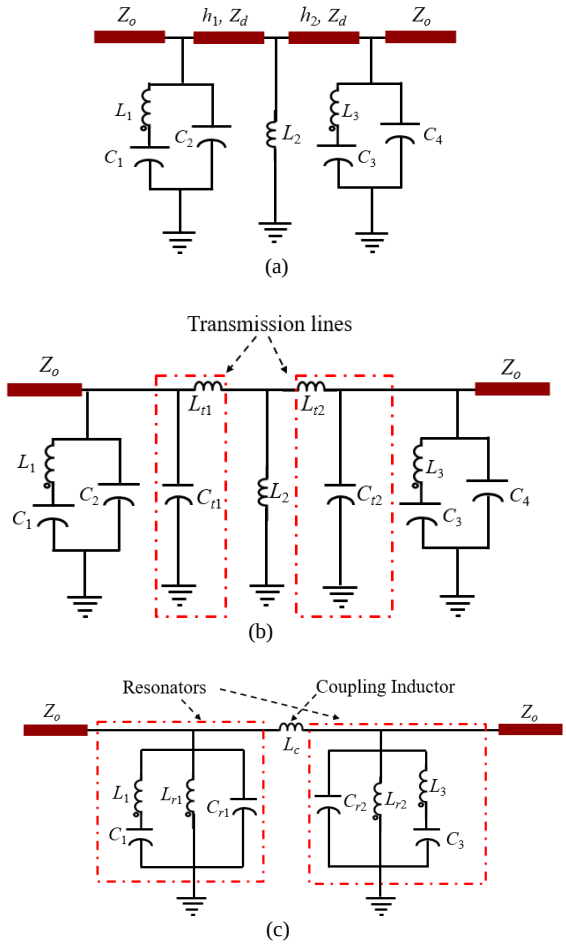

Fig. 2. Equivalent circuit model of the proposed second-order bandpass FSS (a) with transmission lines; (b) using shunt capacitors and series inductors instead of transmission lines; and (c) after star-delta transformation.

The three inductors, L_{t1}, L_2 and L_{t2} in Fig. 2(b) can be transformed into the T-configuration as shown in Fig. 2(c) by using the well-known star-delta transformation [7]. It is assumed that each resonant circuit is coupled only with the circuit adjacent to it. As can be observed, the circuit shown in Fig. 2(c) is composed of two resonators coupled to one another with a single inductor. This circuit presents a second-order coupled-resonator bandpass filter as described in [7]. The resonant frequency can be calculated as [8].

$$f_o \approx \frac{1}{2\pi\sqrt{C_1(C_2+\varepsilon_r\varepsilon_o h/2)(2L_1+2L_2+2\mu_o h)/(C_1+C_2)}} \quad (1)$$

where ε_r and μ_r are the relative permittivity and permeability of the substrate, respectively. It is obvious from (1) that L_1, the inductance of the resonant structure layer, contributes significantly to the miniaturization of the proposed structure. This inductance in the resonant structure (L_1) is designed to have a high value, much stronger than the inductance of the inductive layer to lower the resonant frequency or miniaturize the element size.

The values of the inductors L_{r1}, L_{r2}, and L_1 are related to L_{t1}, L_{t2}, and L_c by: $L_{r1}= L_{t1}+ L_2 (1+ L_{t1}/L_{t2})$ and $L_{r2}= L_{t2}+ L_2 (1+ L_{t2}/L_{t1})$. The coupling inductor $L_c= L_{t1}+ L_2 + (L_{t1}/ L_{t2})/L_2$, while $C_{r1}=C_2+C_{t1}$, $C_{r2}= C_4+C_{t2}$ and. The values of lumped-element components in Fig. 2 (a), to achieve the desired response, can be determined. By taking $C_1= C_3$=0.30 pF, $C_2 =C_4=$ 0.25 pF, $L_1=L_3$ = 2.34 nH and L_2 =0.27 nH, the calculated reflection and transmission coefficients of the equivalent circuit are shown in Fig. 3.

To design the proposed miniaturized FSS with the desired response, one can first determine the values of the elements used in the equivalent circuit model of Fig. 2, then the initial dimensions of these *LC* components can be approximated using the formulas in [9].

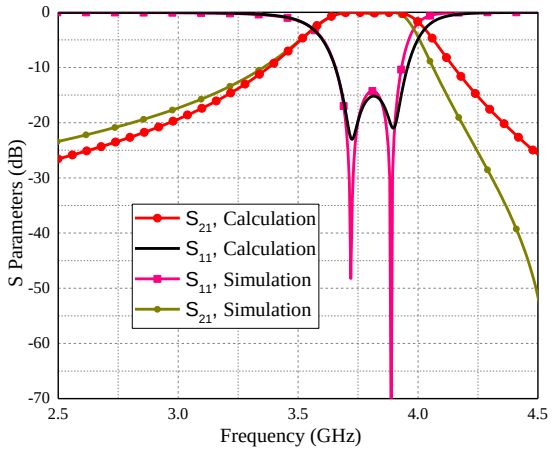

Fig. 3. Comparison between the calculated and simulated transmission and reflection coefficients of the proposed second-order bandpass FSS.

Table I. Physical parameters of an element of the proposed second order bandpass FSS

Parameter	D_x	D_y	h_1	h_2
Value	6 mm	6 mm	1.6 mm	1.6 mm
Parameter	W_s	W_i	W_p	W_l
Value	0.2 mm	2.4 mm	2.3 mm	0.2 mm
Parameter	ε_r	S	g	
Value	4.3	0.1 mm	0.2 mm	

Finally, based on the results obtained from full-wave simulation on the array element of the proposed FSS, the dimensions of the inductive and resonant structures can be tuned to achieve the desired frequency response. The final design parameters of an array element are listed in Table I.

Fig. 4 shows the geometry dimensions of each layer of the proposed FSS after tuning. Each periodic element has

This article has been accepted for publication in a future issue of this journal, but has not been fully edited. Content may change prior to final publication. Citation information: DOI 10.1109/LAWP.2017.2746266, IEEE Antennas and Wireless Propagation Letters

dimensions of D_x and D_y toward the x and y axis, respectively. The period of the inductive layer in x and y direction is D_x and D_y. D_x-s and D_y-s are the dimensions of the resonant structures on the first and the third layers as shown in Fig. 1 and Fig. 4; where s represents the separation between the two adjacent structures. W_p is the width of the square patch. W_i is the width of the cross dipole.

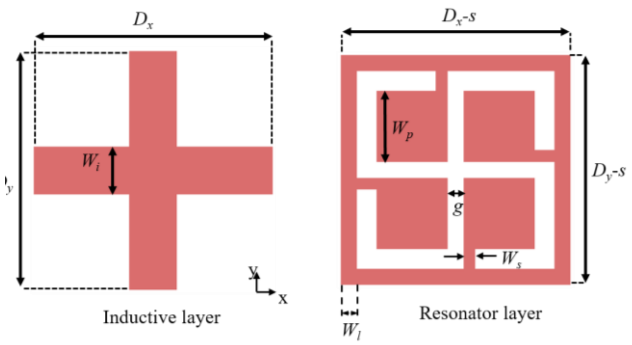

Fig. 4. Top view of the array element of the second-order bandpass FSS. The resonant structure is shown on the right-hand side and the inductive (cross-dipole) layer is shown on the left-hand side.

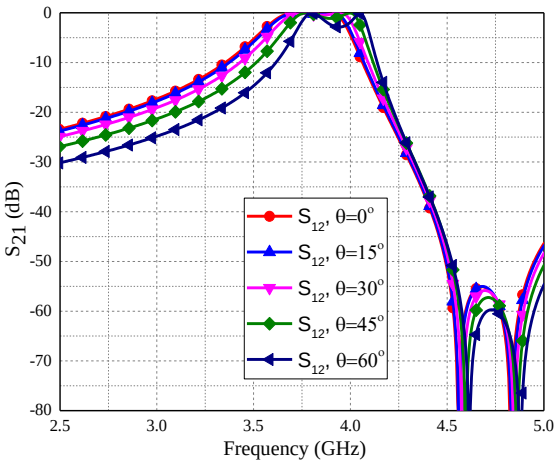

Fig. 5. Simulated transmission coefficients of the proposed second-order FSS with variable incident angles for the TE mode.

Fig. 3 also shows the comparison between the calculated transmission and reflection coefficients and the simulated ones. Fig. 5 and Fig. 6 show the simulated frequency responses of the proposed FSS for the TE and TM modes, respectively. The resonant frequency is 3.8 GHz, and the fractional bandwidth is about 10% at the normal incident angle. The insertion loss is 0.10 dB (assuming a lossless FR4). Whereas, using a lossy FR4 with a loss tangent of 0.019, the simulated insertion loss in the passband is about 1.05 dB. The simulation results also show that the response of the proposed FSS is stable against incident angles. The frequency shift of the FSS at the TE mode with different incident angles is shown in Fig. 5. It can be seen that the center frequency is shifted only by 2.6% from 0˚ to 60˚. The response is stable at the TM mode as well, as shown in Fig. 6. The comparison with other works is shown in Table II. It can be observed that the proposed structure is very stable, especially when the incident angle is high as 60˚. This is expected because FSSs with miniaturized array elements usually exhibit stable responses for oblique incidence.

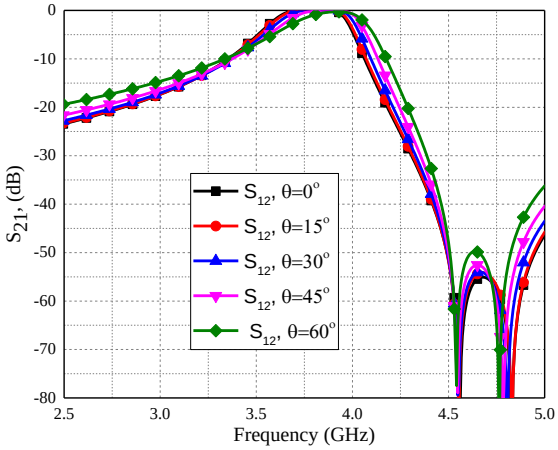

Fig. 6. Simulated transmission coefficients of the proposed second-order FSS with variable incident angles for the TM mode.

Table II. Comparison with other works regarding the center frequency deviations with incident angles

FSS	f_o (GHz)	Incident angle	TE	TM
[2]	10	60°	7%	10%
[4]	21	40°	2.5%	2.3%
[10]	10	60°	18%	16%
This work	3.8	40°	2%	1.8%
This work	3.8	60°	2.6%	2.6%

Table III. Comparison with other works regarding the size, thickness and factional bandwidth (BW) of array elements

FSS	Order	f_o (GHz)	Element size	Overall thickness	BW
[2]	2	10	0.15λ	0.033λ	20%
[3]	2	16.5	0.104 λ	0.22λ	10%
[4]	2	21	0.21 λ	0.273λ	5%
[8]	2	24	0.16 λ	0.033λ	19%
[10]	2	10	0.1λ	0.067λ	21%
[11]	3	8.5	0.2λ	0.257λ	15%
This work	2	3.8	0.076 λ	0.038 λ	10%

Due to symmetry, the frequency response of the proposed structure is independent from the polarization angle. These features offer great flexibility for the proposed structure to be used for many applications.

A comparison of the proposed FSS filter with other reported ones is illustrated in Table III. It can be seen that the proposed structure has the smallest size. The overall thickness is one of the lowest as well. The thickness is only slightly thicker than that in [2] and [8]. However the fractional bandwidth is about half. Had the FSS been designed with the same fractional bandwidth, the thickness would have been thinner than them. This is because, to design an FSS with a wider bandwidth, the coupling between the first and third layers required would be stronger. Hence the substrate could be thinner.

Because of their relatively large size, most traditional high order bandpass FSSs are designed at the X, Ku, K and Ka band, rather than at lower frequencies, as can be observed from Table III. The size of the proposed element is very compact and the overall thickness is small, which make the proposed design very suitable for low frequency applications.

III. Experiment Setup

A prototype of the proposed FSS filter has been fabricated and tested to validate the design method. The fabricated FSS is

shown in Fig. 7. The size of the FSS prototype is 198 mm × 198 mm. It consists of 33 × 33 elements. A vector network analyzer and two horn antennas were used for the measurement. Each antenna is placed 75 cm away from the FSS. The distance is large enough to satisfy the far field condition (meeting $> 2D^2/\lambda$ condition), where D is the antenna aperture size and λ is the wavelength in free space at the resonant frequency. Thus the wave arriving at the FSS can be considered as a plane wave. To avoid spillover or diffraction at the edge of the FSS, RF absorbing materials are used around the edges

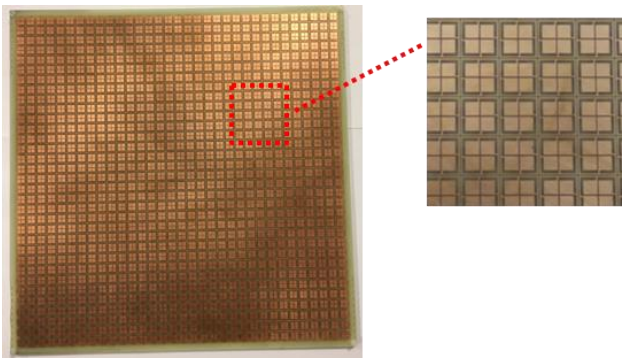

Fig. 7. Photograph of the fabricated prototype of the proposed second-order bandpass FSS.

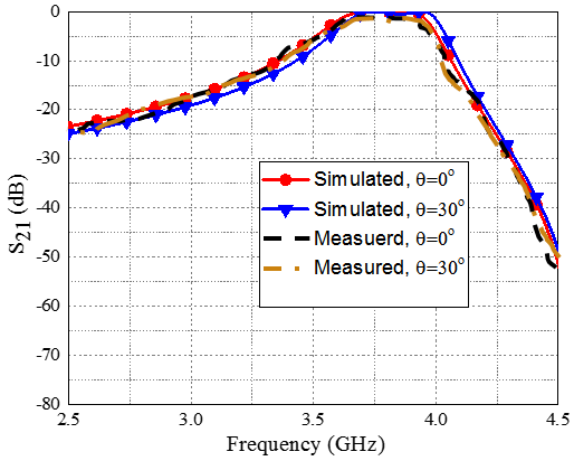

Fig. 8. Simulated and measured responses of the proposed second-order bandpass FSS.

The measurement was done in two steps. First, the transmission coefficient between the two horn antennas was measured without the FSS. Second, the transmission coefficient was measured with the FSS prototype between the antennas. Then the measured transmission with the FSS is normalized with respect to the measured data without the FSS. The transmission coefficient S_{21} was measured at various angles of incidence. The measured results are shown in Fig. 8 for the incident angles of 0˚ and 30˚. They show very good agreement with the simulated ones. As can be observed, the structure exhibits a bandpass response. The center frequency of the passband is 3.8 GHz with a fractional bandwidth of 10%. The frequency response of the proposed FSS is insensitive to the wave incident angle. The FSS was also tested under various polarization angles. The performance is almost independent from polarization angles due to the symmetrical nature of the proposed element.

IV. Conclusion

In this paper, a new approach to design a miniaturized second-order bandpass filter has been proposed. The miniaturized FSS has been built by using a configuration of three surfaces layers. The overall thickness of the proposed structure is 0.038λ, and the element dimensions are 0.076λ × 0.076λ for the prototype, which is one of the smallest reported so far. The miniaturization was realized by using resonant structures on the first and third layers. The proposed technique is particularly useful for low frequency applications. The structure exhibits very good features as an FSS, such as insensitivity to the incident angle and independence from the polarizations. The proposed design method with these features is very attractive for a wide range of applications.

References

[1] B. A. Munk, "Frequency selective surfaces theory and design. john Wiley&Sons," ed: Inc, 2000.

[2] M. Al-Joumayly and N. Behdad, "A new technique for design of low-profile, second-order, bandpass frequency selective surfaces," *IEEE Trans. Antennas Propag.*, vol. 57, pp. 452-459, 2009.

[3] M. Gao, S. M. A. M. H. Abadi, and N. Behdad, "A Dual-Band, Inductively Coupled Miniaturized-Element Frequency Selective Surface With Higher Order Bandpass Response," *IEEE Trans. Antennas Propag.*, vol. 64, pp. 3729-3734, 2016.

[4] S. M. A. M. H. Abadi and N. Behdad, "Inductively-coupled miniaturized-element frequency selective surfaces with narrowband, high-order bandpass responses," *IEEE Trans. Antennas Propag.*, vol. 63, pp. 4766-4774, 2015.

[5] M. Hussein, J. Zhou, Y. Huang, A. Sohrab, and M. Kod, "Frequency selective surface with simple configuration stepped-impedance elements," *Antennas Propag., EuCAP*, Davos, pp.1-4, 2016.

[6] R. W. P. King, *Fundamental electromagnetic theory*: Dover Publications, 1963.

[7] A. I. Zverev, *Handbook of filter synthesis*: Wiley-Blackwell, 2005.

[8] M. Salehi and N. Behdad, "A second-order dual X-/Ka-band frequency selective surface," *IEEE Microwave Wireless Components Lett.*, vol. 18, pp. 785-787, 2008.

[9] N. Marcuvitz, *Waveguide handbook*, ser. MIT Rad. Lab., New York: McGraw-Hill, vol. 10, 1951.

[10] M. Yan, S. Qu, J. Wang, A. Zhang, L. Zheng, Y. Pang, *et al.*, "A miniaturized dual-band FSS with second-order response and large band separation," *IEEE Antennas Wireless Propag. Lett.*, vol. 14, pp. 1602-1605, 2015.

[11] M. Gao, S. M. A. M. H. Abadi, and N. Behdad, "A Hybrid Miniaturized-Element Frequency Selective Surface With a Third-order Bandpass Response," *IEEE Antennas Wireless Propag. Lett.*, vol. 16, pp. 708 - 7011, 2016.